Wind and Structures, *Vol. 19, No. 5 (2014) 481-503*
DOI: http://dx.doi.org/10.12989/was.2014.19.5.481

Theoretical investigation on rain-wind induced vibration of a continuous stay cable with given rivulet motion

Li Shouying[*1], Chen Zhengqing[1a] and Li Shouke[2b]

[1]Wind Engineering Research Center, Hunan University, Yuelu Hill, Changsha, 410082, China
[2]School of Civil Engineering, Hunan University of Science and Technology, Xiangtan, 411201, China

(Received September 24, 2013, Revised June 9, 2014, Accepted August 20, 2014)

Abstract. A new theoretical model on rain-wind induced vibration (RWIV) of a continuous stay cable is developed in this paper. Different from the existing theoretical analyses in which the cable was modeled as a segmental rigid element, the proposed scheme focuses on the in-plane and out-of-plane responses of a continuous stay cable, which is identical with the prototype cable on cable-stayed bridge. In order to simplify the complexities, the motion law of the rivulet on the cable surface is assumed as a sinusoidal way according to some results obtained from wind tunnel tests. Quasi-steady theory is utilized to determine the aerodynamic forces on the cable. Equations of motion of the cable are derived in a Cartesian Coordinate System and solved by using finite difference method to obtain the in-plane and out-of-plane responses of the cable. The results show that limited cable amplitudes are achieved within a limited range of wind velocity, which is a unique characteristic of RWIV of stay cable. It appears that the in-plane cable amplitude is much larger than the out-of-plane cable amplitude. Rivulet frequency, rivulet distribution along cable axis, and mean wind velocity profile, all have significant effects on the RWIV responses of the prototype stay cable. The effects of damping ratio on RWIVs of stay cables are carefully investigated, which suggests that damping ratio of 1% is needed to well mitigate RWIVs of prototype stay cables.

Keywords: a continuous stay cable; rain-wind induced vibration; mechanism study; finite difference method; theoretical model

1. Introduction

In the 1980's, the stay cables on the MekoNishi Bridge in Japan oscillated violiently with large amplitude under the combined action of wind and rain, but no vibration was found only under the action of wind. This phenomenon could not be explained clearly by the existing theories at that time. Hikami and Shiraishi (1988) conducted a 5-month field observation on the MekoNishi Bridge and carried out a series of wind tunnel tests to recur it, and named it rain-wind induced vibration (RWIV). Since that time, the studies on the mechanism of RWIVs of stay cables became one of the main research subjects in bridge engineering community. Three main means, including field observations (Hikami and Shiraishi 1988, Matsumoto *et al*. 1990, Chen *et al*. 2004), wind

∗Corresponding author, Associate professor, E-mail: shyli@hnu.edu.cn
[a] Professor, E-mail: zqchen@hnu.edu.cn
[b] Assistant Professor, E-mail: lishouke@hnust.edu.cn

Copyright © 2014 Techno-Press, Ltd.
http://www.techno-press.org/?journal=was&subpage=8 ISSN: 1226-6116 (Print), 1598-6225 (Online)

tunnel tests (Hikami and Shiraishi 1988, Yamaguchi 1990, Gu *et al*. 2002, Gu and Du 2005, Li *et al*. 2010) and theoretical analyses (Yamaguchi 1990, Gu and Lu 2001, Peil and Nahrath 2003, Burgh and Hartono 2003, Xu and Wang 2003, Wilde and Witkowski 2003, Cosentino *et al*. 2003, Cao *et al*. 2003, Gu *et al*. 2009, Gu 2009, Li *et al*. 2013), were adopted. Recently, with the developments of computer hardware and Computational Fluid Dynamics (CFD) method, numerical simulation has been gradually applied in the mechanism investigation of RWIV of stay cable (Rocchi and Zasso 2002, Li and Gu 2006, Taylor and Robertson 2011).

Currently, two types of explanations have been advanced. The first, shared by most investigators, postulates that the rivulet formed on the upper surface of cable, which alters the flow near the cable, is the key factor for the onset and sustenance of RWIV. The second viewpoint is advanced by Matsumoto (1995) which is based on the field observations of the role of axial flow along the cable axis on RWIV. These vibrations were observed to take place at even higher reduced wind speeds of 20, 40, 60, 80.

The first theoretical analysis model of RWIV was established by Yamaguchi (1990) in which both the natural frequency of the rivulet and modal aerodynamic damping of the cable with the rivulet were analyzed. In this model, the cable and the rivulet were treated as a unit, which means it was not necessary to evaluate the forces on the rivulet. There was little progress in theoretical analyses of RWIV in the 1990's. In order to simplify the over complexity, some researchers (Xu and Wang 2003, Wilde and Witkowski 2003, Burgh and Hartono 2003) assumed a sinusoidal oscillation of the rivulet for analyzing RWIV. The range of wind velocity over which the RWIVs take place was established by invoking an additional assumption concerning the relationship between the rivulet equilibrium position and the wind velocity. Gu and Lu (2001) established equations of motion for both the cable and the upper rivulet by assuming that the aerodynamic force on the rivulet was proportional to the torsional force on the cable with the rivulet, while the interaction force between cable surface and rivulet was set to zero. Peil and Nahrath (2003a) put forward a theoretical model including in-plane and out-of-plane degree-of-freedom of the cable and a tangential degree-of-freedom of the rivulet. They assumed the interaction between the cable surface and the rivulet to be modeled by a linear damping force. The focus of their study, however, was only on nonlinear stability and bifurcation of the system. Peil *et al*. (2003b) extended their study by including the lower rivulet. Cao *et al*. (2003) treated the rivulet oscillations as a stochastic process, and assumed the interaction between the cable surface and the rivulet to be modeled by a restoring force and a linear damping force. Gu *et al*. (2009) carried out wind tunnel tests to obtain the aerodynamic forces acting on the cable and the upper rivulet, and established a theoretical model, in which the in-plane degree-of-freedom of the cable and the tangential degree-of-freedom of the rivulet were taken into account. In this model, the interaction between the cable surface and the rivulet was assumed to be a combination of a Coulomb damping force and a linear damping force, while the coupled oscillations of the cable and the upper rivulet were discussed in detail in order to explain the RWIV (Li *et al*. 2008). On the base of Gu *et al*. (2009), Li *et al*. (2013) built a new theoretical model to analyze the interaction between the in-plane and out-of-plane vibrations of stay cable, and wider wind velocity zone in which RWIV takes place was found.

All of the above mentioned theoretical analyses aimed to model a continuous stay cable as a segmental rigid element with one or two degree-of-freedoms, which was usually utilized in wind tunnel tests for the recurrence of RWIV (Hikami and Shiraishi 1988, Gu and Du 2005). These kinds of cable models can reflect some of the characteristics of RWIV to some extent. In fact, the variation of wind speed with height, which significantly affects the formulation and position of the upper rivulet, could not be taken into account in the segmental rigid cable model (Gu 2009). Based on a taut cable model, Zhou and Xu (2007) analytically investigated the RWIV responses of a continuous cable, in which the variation of mean wind speed along the stay cable and the effect of mode shapes of cable motion could be taken in account. However, only the responses of the first natural frequency were analyzed in detail. Xu *et al*. (2008) presents a framework for estimating occurrence probability of RWIV of stay cable, in which the continuous sag cable was simplified as a taut cable. However, different modes of vibrations were found on prototype stay cables, and the RWIVs can transfer from one mode to another mode (Chen *et al*. 2004) in field observations.

In this paper, a new theoretical model on RWIV of a continuous stay cable was established. In order to simplify this complicated problem, the motion of the rivulet was assumed to be sinusoidal. The in-plane and out-of-plane degree-of-freedoms of the cable as well as the cable sag were considered in the present model. Finite difference method was adopted to solve the equations of motion to obtain the responses of prototype stay cable. Taking Cable A20 of the No.2 Nanjing Bridge over Yangtze River as an example, the classical galloping responses of stay cable were firstly studied by fixing the rivulet on the cable surface. Then the effects of wind velocity, rivulet frequency, mean wind velocity profile and cable damping to RWIV responses of the prototype stay cable were investigated in detail.

2 Equations of motion

The following assumptions are made:

(1) Quasi-steady assumption is utilized to evaluate wind forces on the cable attached with upper rivulet. It is acceptable because the frequency of vortex shedding is much higher than the natural frequency of stay cable when RWIVs of stay cables take place.

(2) Only the upper rivulet is taken in account. According to the results of wind tunnel tests (Hikami and shiraishi 1988), lower rivulet has little influence on RWIVs of stay cables.

(3) It is assumed that the shape of the upper rivulet does not change when it oscillates on the cable surface. In fact, the rivulet's shape changes during RWIVs take place, but some studies (Yamaguchi 1990, Li *et al*. 2013) have found that its shape has little effects on the onset of RWIVs of stay cables.

(4) The rivulet oscillation is assumed to obey a sinusoidal way according to the results of field observations and wind tunnel tests (Xu and Wang 2003, Wilde and Witkowski 2003, Li *et al.* 2013).

(5) The effects of axial flow are neglected because it is difficult to exactly evaluate it.

(6) The flexural rigidity, torsional and shear stiffness of stay cable are neglected.

(7) Constitutive relation of stay cable follows Hook's Law, and the stresses on cable section are uniform.

A continuous stay cable with an inclined angle of α is considered, as indicated in Fig. 1. Two end points, the higher point O on the pylon and the lower point A on the deck, have a horizontal distance of L and a vertical distance of R. A Cartesian coordinate system, $Oxyz$, is defined, as shown in Fig. 1. In which, x and z axes are both horizontal, y axis is vertical, the stay cable locates in the plane Oxy. Under the action of gravity, the stay cable exhibits a static profile, which can be expressed by a function $y=f(x)$. The equations governing the motion of the cable can be written as (Irvine 1981)

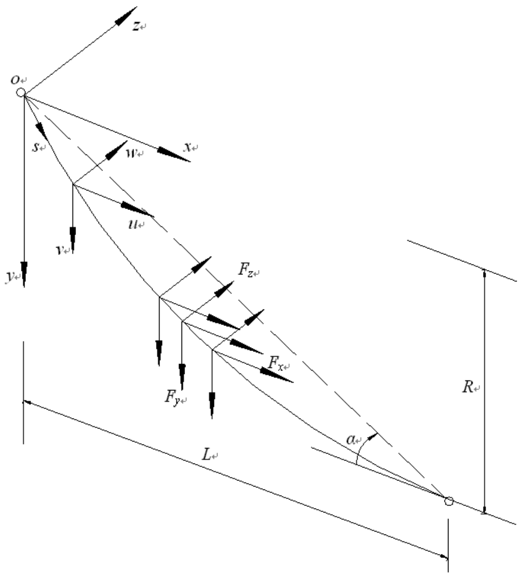

Fig. 1 3-D continuous stay cable with sag

$$\frac{\partial}{\partial s}\left[(T+\tau)(\frac{dx}{ds}+\frac{\partial u}{\partial s})\right]+F_x(x,t)=M\frac{\partial^2 u}{\partial t^2}+c_1\frac{\partial u}{\partial t} \tag{1}$$

$$\frac{\partial}{\partial s}\left[(T+\tau)(\frac{dy}{ds}+\frac{\partial v}{\partial s})\right]+F_y(x,t)=M\frac{\partial^2 v}{\partial t^2}+c_1\frac{\partial v}{\partial t}-Mg \tag{2}$$

$$\frac{\partial}{\partial s}\left[(T+\tau)\frac{\partial w}{\partial s}\right]+F_z(x,t)=M\frac{\partial^2 w}{\partial t^2}+c_2\frac{\partial w}{\partial t} \tag{3}$$

in which, T is the static cable tension only under the action of gravity; τ is the dynamic cable tension under the action of wind; t is the time; u, v and w are the dynamic displacement components in the x, y and z directions, respectively; y is the cable static profile, which will be discussed in section 3.1; s is the curvilinear coordinate; F_x (x, t), F_y (x, t), F_z (x, t) are the aerodynamic forces per unit length in the x, y and z directions, respectively; M is the cable mass per unit length; c_1, c_2 are the in-plane and out-of-plane linear structural damping coefficients of the stay cable, respectively; g is the acceleration of gravity.

Introducing the following transformations (Irvine 1981)

$$\frac{\partial}{\partial s}=\frac{1}{\sqrt{1+[f'(x)]^2}}\frac{\partial}{\partial x} \tag{4a}$$

$$H = T\frac{dx}{ds} \tag{4b}$$

$$h = \tau\frac{dx}{ds} \tag{4c}$$

$$\frac{d}{ds}(T\frac{dy}{ds}) = -Mg \tag{4d}$$

and considering the equations of static profile of the cable, Eqs. (1), (2) and (3) can be rewritten as

$$\frac{1}{\sqrt{1+[f'(x)]^2}}\frac{\partial}{\partial x}\left[(H+h)(1+\frac{\partial u}{\partial x})\right] + F_x(x,t) = M\frac{\partial^2 u}{\partial t^2} + c_1\frac{\partial u}{\partial t} \tag{5}$$

$$\frac{1}{\sqrt{1+[f'(x)]^2}}\frac{\partial}{\partial x}\left[(H+h)\frac{\partial v}{\partial x} + hf'(x)\right] + F_y(x,t) = M\frac{\partial^2 v}{\partial t^2} + c_1\frac{\partial v}{\partial t} \tag{6}$$

$$\frac{1}{\sqrt{1+[f'(x)]^2}}\frac{\partial}{\partial x}\left[(H+h)\frac{\partial w}{\partial x}\right] + F_z(x,t) = M\frac{\partial^2 w}{\partial t^2} + c_2\frac{\partial w}{\partial t} \tag{7}$$

in which, H is the horizontal component of the static cable tension in the x-y plane under the action of gravity, which does not change along the cable axis; h is the horizontal component of the dynamic cable tension under the action of wind; $f'(x)$ is the derivative of cable static profile y with respect to x.

The relationship between the dynamic cable tension, τ, and dynamic cable displacement in the Lagrangian Coordinate can be expressed as (Irvine 1981)

$$\tau = EA\frac{d\bar{s} - ds}{ds} \tag{8}$$

where, E is the cable modulus of elasticity; A is the area of the cable cross section; $d\bar{s}$ and ds are the arc-lengths of the deformed and undeformed cable segments, respectively. According to geometrical relationship (Irvine 1981), we have

$$ds = dx + dy \tag{9}$$

$$d\bar{s}^2 = (dx+\partial u)^2 + (dy+\partial v)^2 + \partial w^2 \tag{10}$$

By combining Eqs. (4), (9) and (10), the horizontal dynamic cable tension h can be expressed as

$$h = \frac{EA}{(1+[f'(x)]^2)^{3/2}} \times \left\{\frac{\partial u}{\partial x} + f'(x)\frac{\partial v}{\partial x} + \frac{1}{2}\left[(\frac{\partial u}{\partial x})^2 + (\frac{\partial v}{\partial x})^2 + (\frac{\partial w}{\partial x})^2\right]\right\} \tag{11}$$

Note that small-amplitude vibration is considered in this study, high order terms in Eq. (11) can be neglected. Eq. (11) can be rewritten as

$$h = \frac{EA}{(1+y_x^2)^{3/2}}\left[\frac{\partial u}{\partial x} + y_x \frac{\partial v}{\partial x}\right] \tag{12}$$

Substituting Eq. (12) into Eqs. (5), (6) and (7) and neglecting the differentials of high order

$$\frac{1}{\sqrt{1+[f'(x)]^2}}\frac{\partial}{\partial x}[(H+\frac{EA}{(1+[f'(x)]^2)^{3/2}})\frac{\partial u}{\partial x}+\frac{EAf'(x)}{(1+[f'(x)]^2)^{3/2}}\frac{\partial v}{\partial x}]+F_x(x,t)=M\frac{\partial^2 u}{\partial t^2}+c_1\frac{\partial u}{\partial t} \tag{13}$$

$$\frac{1}{\sqrt{1+[f'(x)]^2}}\frac{\partial}{\partial x}[(H+\frac{EA[f'(x)]^2}{(1+[f'(x)]^2)^{3/2}})\frac{\partial v}{\partial x}+\frac{EAf'(x)}{(1+[f'(x)]^2)^{3/2}}\frac{\partial u}{\partial x}]+F_y(x,t)=M\frac{\partial^2 v}{\partial t^2}+c_1\frac{\partial v}{\partial t} \tag{14}$$

$$\frac{1}{\sqrt{1+[f'(x)]^2}}\frac{\partial}{\partial x}\left[H\frac{\partial w}{\partial x}\right]+F_z(x,t)=M\frac{\partial^2 w}{\partial t^2}+c_2\frac{\partial w}{\partial t} \tag{15}$$

3. Details of equations

3.1 Cable static profile

For an inclined sagged cable, its exact static profile should be category curve if the cable mass is uniform (Irvine 1981). However, the stay cables on cable-stayed bridges have small sag-span ratio, for example, less than 1%. Ren and Gu (2005) found that the category static profile of stay cables on cable-stayed bridges can be well approximated by parabolic curve. For a Cartesian coordinate system indicated in Fig. 2, the static profile can be expressed as (Ren and Gu 2005)

$$y = f(x) = -\frac{Mg}{2H}\sec\alpha x^2 + \frac{1}{2}(\frac{MgL}{H}\sec\alpha + 2\tan\alpha)x \tag{16}$$

where, α is the inclined angle. $f'(x)$ in Eqs. (13)-(15) can be obtained from Eq. (16)

$$f'(x) = \frac{MgL}{2H}\sec\alpha + \tan\alpha - (\frac{Mg}{H}\sec\alpha)x \tag{17}$$

Eq. (17) indicates that the values of $f'(x)$ at the upper end (x=0), middle point (x=L/ 2) and lower end (x=L) of stay cable respectively equal to

$$f'(x) = \begin{cases} \tan\alpha + \dfrac{MgL}{2H}\sec\alpha & x = 0 \\ \tan\alpha & x = L/2 \\ \tan\alpha - \dfrac{MgL}{2H}\sec\alpha & x = L \end{cases} \tag{18}$$

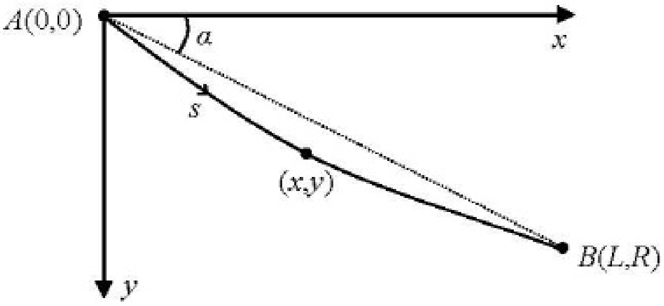

Fig. 2 Cable static profile

3.2 Aerodynamic forces of stay cable

Theoretical analyses based on segmental rigid cable model demonstrated that the mechanism of RWIVs of stay cables are somewhat like galloping except that the rivulet moves up and down upon the cable surface (Yamaguchi 1990, Li *et al*. 2013). Consequently, it is acceptable to describe the aerodynamic forces on the cable by using quasi-steady theory (Holmes 2003). The orientation of stay cable can be defined by the inclined angle α and the yaw angle β, as shown in Fig. 3.

A horizontal wind velocity U_0 in Fig. 3 can be decomposed into a component perpendicular to cable plane and a component parallel to cable axis (Wilde and Witkowski 2003). In this paper, the effects of axial flow are neglected. The wind velocity component perpendicular to cable plane, U, can be expressed as

$$U = U_0\sqrt{\cos^2\beta + \sin^2\alpha\sin^2\beta} = U_0\sqrt{\sin^2\alpha + \cos^2\alpha\cos^2\beta} \tag{19}$$

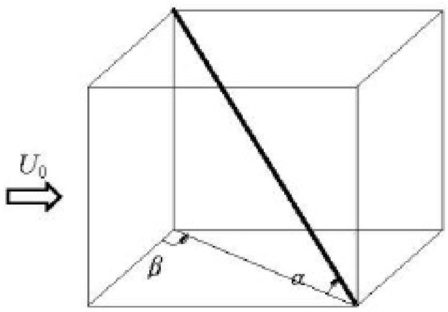

Fig. 3 Inclined angle α and yaw angle β of stay cable

and the angle between U and horizontal line, γ, can be determined from

$$\gamma = \arcsin\left(\frac{\sin\alpha\sin\beta}{\sqrt{\cos^2\beta + \sin^2\alpha\sin^2\beta}}\right) \tag{20}$$

Considering the cable vertical vibration, $\dot{y}$, a relative wind velocity to the cable can be expressed as

$$U_{rel} = \sqrt{(U\cos\gamma)^2 + (U\sin\gamma + \dot{y})^2} \tag{21}$$

and the angle between U and U_{rel} is

$$\phi = \arctan\left(\frac{\dot{y} + U\sin\gamma}{U\cos\gamma}\right) \tag{22}$$

the angle between U_{rel} and horizontal line is

$$\phi' = \phi + \theta_0 + \theta \tag{23}$$

where, θ_0 is the rivulet equilibrium position; θ is the rivulet displacement away from the balance position. θ_0 and θ will be discussed in Section 3.3.

The spatial relationships between stay cable, rivulet and wind direction are shown in Fig. 4. Based on Quasi-steady theory, the aerodynamic forces on stay cable with rivulet can be obtained from

$$F_x(x,t) = \frac{1}{2}\rho D U_0^2 [C_L(\phi')\cos(\phi) + C_D(\phi')\sin\phi]\sin\alpha \tag{24}$$

$$F_y(x,t) = -\frac{1}{2}\rho D U_0^2 [C_L(\phi')\cos(\phi) + C_D(\phi')\sin\phi]\cos\alpha \tag{25}$$

$$F_z(x,t) = \frac{1}{2}\rho D U_0^2 [-C_L(\phi')\sin(\phi) + C_D(\phi')\cos\phi] \tag{26}$$

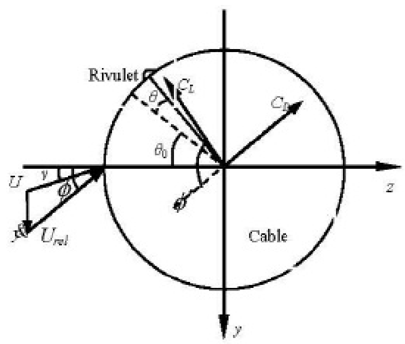

Fig. 4 Spatial relationships between stay cable, rivulet and wind direction

in which, ρ is the air density; D is the diameter of stay cable; C_D and C_L are the mean drag and lift coefficients of stay cable attached with rivulet, respectively. The results of C_D and C_L from Gu *et al*. (2009) by using wind tunnel tests (as shown in Fig. 5) and from Li and Gu (2006) by using CFD simulations (as shown in Fig. 6) are both adopted. It should be noted that the orientation of stay cable are limited to α=30° and β=35° in the present paper.

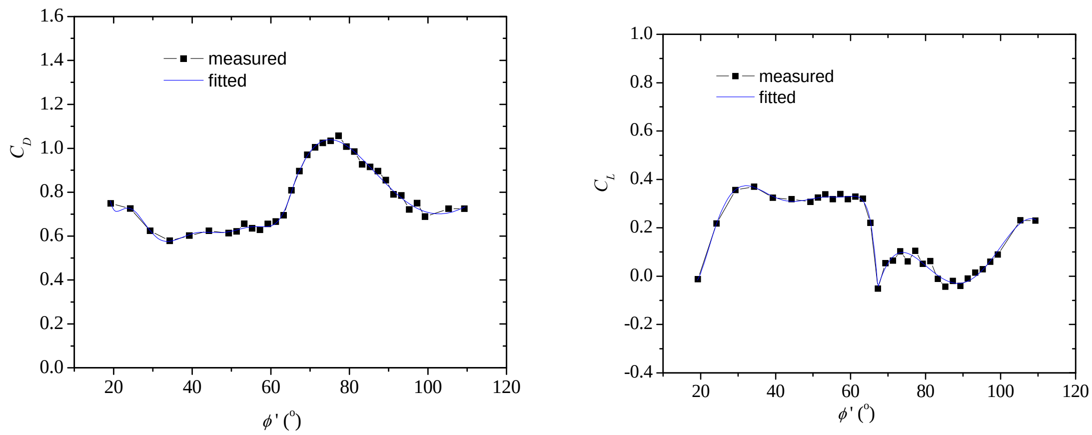

Fig. 5 The mean drag and lift coefficients from Gu *et al*. (2009) by using wind tunnel test (α=30°, β=35°)

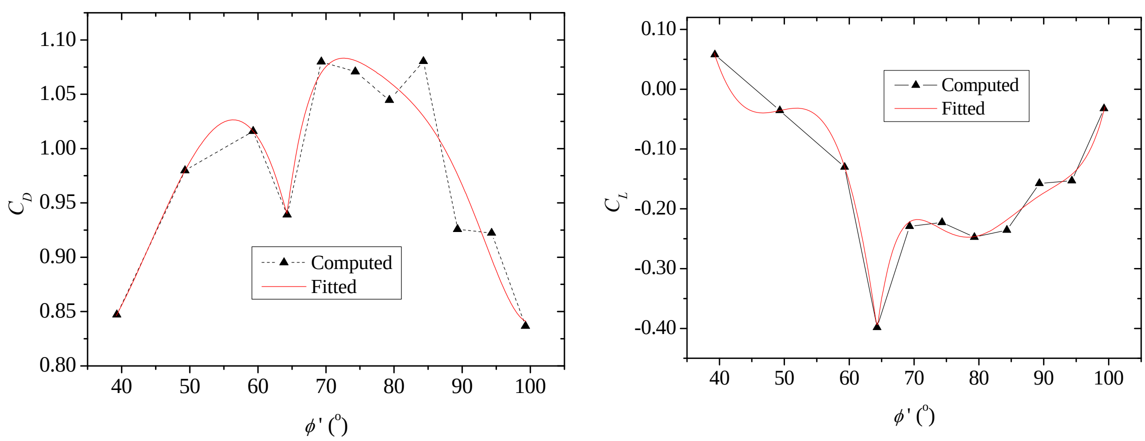

Fig. 6 The mean drag and lift coefficients from Li and Gu (2006) by using CFD simulations (α=30°, β=35°)

3.3 Motion law of rivulet

In field observations on RWIVs of stay cables, the rivulet was found to move up and down on the cable surface, but it is difficult to survey the exact motion law of the rivulet in situ. Several researchers made efforts to measure the rivulet motion law in wind tunnel tests (Hikami and Shiraishi 1988, Gu and Du 2005, Li *et al*. 2010). The results measured by Gu and Du (2005) was adopted in this paper. For cable orientation of α=30° and β=35°, the relationship between rivulet balance position θ_0 and wind velocity U_0 is

$$\theta_0 = 90 - (365.4807 \times \exp(-U_0/2.3186) + 6.9787) \tag{27}$$

The rivulet displacement away from the balance position θ_0 is assumed as

$$\theta = a_m \sin \omega t \tag{28}$$

where, a_m is the one-side amplitude of the rivulet; ω is the rivulet frequency; t is the time. In the existing theoretical analyses on segmental rigid cable models (Xu and Wang 2003, Wilde and Witkowski 2003), the rivulet frequency was assumed to be equal to the natural frequency of segmental cable model. However, there are lots of natural frequencies for a prototype stay cable. Consequently, a parametric analysis about rivulet frequency will be conducted to evaluate its effects in the present paper.

a_m is assumed to be (Gu and Du 2005)

$$a_m(U_0) = a_1 \exp\left(-\frac{(U_0 - U_{\max})^2}{a_2}\right) \tag{29}$$

where, a_1, a_2 and U_{max} are respectively equal to 10.0, 13.9 and 8.5.

4. Finite difference method

Finite Difference Method is adopted to solve Eqs. (13)-(15), which can be re-written as

$$A_1 \frac{\partial^2 u}{\partial x^2} + A_2 \frac{\partial^2 v}{\partial x^2} + A_3 \frac{\partial u}{\partial x} + A_4 \frac{\partial v}{\partial x} + F_x(x,t) = m \frac{\partial^2 u}{\partial t^2} + c_1 \frac{\partial u}{\partial t} \tag{30}$$

$$A_5 \frac{\partial^2 v}{\partial x^2} + A_2 \frac{\partial^2 u}{\partial x^2} + A_6 \frac{\partial v}{\partial x} + A_4 \frac{\partial u}{\partial x} + F_y(x,t) = m \frac{\partial^2 v}{\partial t^2} + c_1 \frac{\partial v}{\partial t} \tag{31}$$

$$A_7 \frac{\partial^2 w}{\partial x^2} + F_z(x,t) = m \frac{\partial^2 w}{\partial t^2} + c_2 \frac{\partial w}{\partial t} \tag{32}$$

in which

$$A_1 = \frac{H}{\sqrt{1+y_x^2}} + \frac{EA}{(1+y_x^2)^2} \qquad A_2 = \frac{EAy_x}{(1+y_x^2)^2} \qquad A_3 = -\frac{3EAy_x}{(1+y_x^2)^3}\frac{\partial^2 y}{\partial x^2}$$

$$A_4 = \frac{EA(1-2y_x^2)}{(1+y_x^2)^3}\frac{\partial^2 y}{\partial x^2} \qquad A_5 = \frac{H}{\sqrt{1+y_x^2}} + \frac{EAy_x^2}{(1+y_x^2)^2} \qquad A_6 = \frac{EA(2y_x - y_x^3)}{(1+y_x^2)^3}\frac{\partial^2 y}{\partial x^2}$$

$$A_7 = \frac{H}{\sqrt{1+y_x^2}}$$

Two ends of stay cable, attached to the deck and the tower, are both assumed to no vibrations, and the stay cable keep stationary at the initial time. Boundary conditions and initial conditions for Eqs. (30)- (32) are

$$\begin{cases} u(0,t) = v(0,t) = w(0,t) = 0; u(L,t) = v(L,t) = w(L,t) = 0 & t \in (0,T) \\ u(x,0) = v(x,0) = w(x,0) = 0; \dfrac{\partial u(x,0)}{\partial t} = \dfrac{\partial v(x,0)}{\partial t} = \dfrac{\partial w(x,0)}{\partial t} = 0 & x \in (0,L) \end{cases} \tag{33}$$

The cable is discretized into N segmentations in space (as shown in Fig. 7) and M segmentations in time. Space node is j=0, 1, 2, …, N and the distance between the adjacent space nodes along x direction, h, equals to L/N. Time node is k=0, 1, 2, …, M and the distance between the adjacent time nodes, τ, equals to T/M, in which T is the total computational time.

Two order central difference is used

$$\frac{\partial^2 u}{\partial x^2}\Big|_j^k = \frac{1}{h^2}(u_{j-1}^k - 2u_j^k + u_{j+1}^k) + o(h^2) \tag{34a}$$

$$\frac{\partial^2 v}{\partial x^2}\Big|_j^k = \frac{1}{h^2}(v_{j-1}^k - 2v_j^k + v_{j+1}^k) + o(h^2) \tag{34b}$$

$$\frac{\partial^2 w}{\partial x^2}\Big|_j^k = \frac{1}{h^2}(w_{j-1}^k - 2w_j^k + w_{j+1}^k) + o(h^2) \tag{34c}$$

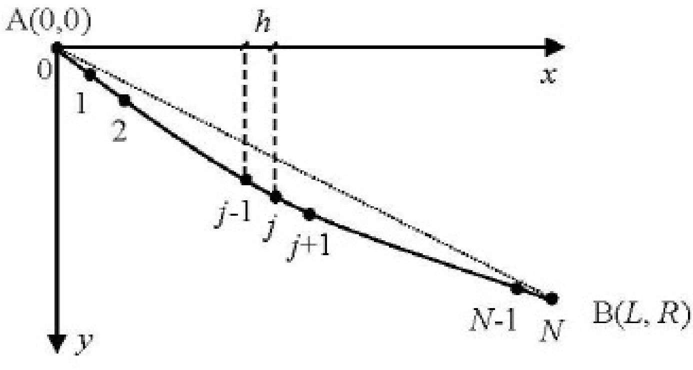

Fig. 7 Space discretization of stay cable

$$\frac{\partial^2 u}{\partial t^2}\Big|_j^k = \frac{1}{\tau^2}(u_j^{k-1} - 2u_j^k + u_j^{k+1}) + o(\tau^2) \tag{34d}$$

$$\frac{\partial^2 v}{\partial t^2}\Big|_j^k = \frac{1}{\tau^2}(v_j^{k-1} - 2v_j^k + v_j^{k+1}) + o(\tau^2) \tag{34e}$$

$$\frac{\partial^2 w}{\partial t^2}\Big|_j^k = \frac{1}{\tau^2}(w_j^{k-1} - 2w_j^k + w_j^{k+1}) + o(\tau^2) \tag{34f}$$

$$\frac{\partial u}{\partial t}\Big|_j^k = \frac{1}{2\tau}(u_j^{k+1} - u_j^{k-1}) + o(\tau^2) \tag{34g}$$

$$\frac{\partial v}{\partial t}\Big|_j^k = \frac{1}{2\tau}(v_j^{k+1} - v_j^{k-1}) + o(\tau^2) \tag{34h}$$

$$\frac{\partial w}{\partial t}\Big|_j^k = \frac{1}{2\tau}(w_j^{k+1} - w_j^{k-1}) + o(\tau^2) \tag{34i}$$

$$\frac{\partial u}{\partial x}\Big|_j^k = \frac{1}{2h}(u_{j+1}^k - u_{j-1}^k) + o(h^2) \tag{34j}$$

$$\frac{\partial v}{\partial x}\Big|_j^k = \frac{1}{2h}(v_{j+1}^k - v_{j-1}^k) + o(h^2) \tag{34k}$$

in which, u_j^k, v_j^k, w_j^k represent the values of u, v, w at space node j and time node k. Substituting Eq. (34) into Eqs. (30)-(33), difference scheme can be obtained

$$\begin{aligned} u_j^{k+1} = \frac{1}{(\frac{m}{\tau^2} + \frac{c_1}{2\tau})}&[(\frac{A_1}{h^2} + \frac{A_3}{2h})u_{j+1}^k + (\frac{2m}{\tau^2} - \frac{2A_1}{h^2})u_j^k + (\frac{A_1}{h^2} - \frac{A_3}{2h})u_{j-1}^k \\ &+ (\frac{c_1}{2\tau} - \frac{m}{\tau^2})u_j^{k-1} + A_2\frac{v_{j+1}^k - 2v_j^k + v_{j-1}^k}{h^2} + A_4\frac{v_{j+1}^k - v_{j-1}^k}{2h} \\ &+ F_x(x_j, t_k)] \end{aligned} \tag{35}$$

$$\begin{aligned} v_j^{k+1} = \frac{1}{(\frac{m}{\tau^2} + \frac{c_1}{2\tau})}&[(\frac{A_5}{h^2} + \frac{A_6}{2h})v_{j+1}^k + (\frac{2m}{\tau^2} - \frac{2A_5}{h^2})v_j^k + (\frac{A_5}{h^2} - \frac{A_6}{2h})v_{j-1}^k \\ &+ (\frac{c_1}{2\tau} - \frac{m}{\tau^2})v_j^{k-1} + A_2\frac{u_{j+1}^k - 2u_j^k + u_{j-1}^k}{h^2} + A_4\frac{u_{j+1}^k - u_{j-1}^k}{2h} \\ &+ F_y(x_j, t_k)] \end{aligned} \tag{36}$$

$$w_j^{k+1} = \frac{1}{(\frac{m}{\tau^2} + \frac{c_2}{2\tau})}[\frac{A_7}{h^2} w_{j+1}^k + (\frac{2m}{\tau^2} - \frac{2A_7}{h^2})w_j^k + \frac{A_7}{h^2} w_{j-1}^k + (\frac{c_2}{2\tau} - \frac{m}{\tau^2})w_j^{k-1} + F_z(x_j, t_k)] \tag{37}$$

(j=1,2,3,4,……,N-1 , k=1,2,3,4,……M)

Eqs. (35)-(37) indicate an explicit difference scheme from which the values of u, v and w at the time k+1 (u^{k+1}, v^{k+1} and w^{k+1}) can be determined directly from the values at the time k and k-1. This means that only algebraic operations, instead of solving equation sets, should be carried out to obtain the responses of stay cable.

5 Results and discussions

A cable numbered A20 of the No.2 Nanjing Bridge over Yangtze River, on which large amplitudes of RWIVs are observed in situ, is taken as an example. The cable length is 330.4 m; the mass per unit length is 81.167 kg/m; the sectional area is 0.0102 m^2; the design tension is 6403 kN; the Young's modulus is 1.9×10^{11} N/m^2; The fundamental natural frequency is 0.415 Hz; c_1 and c_2 are respectively assumed to be 0.1% and 0.05%; the inclined angle and yaw angle are respectively 30º and 35º. C_D and C_L of stay cable attached with artificial rivulet reported in Gu *et al*. (2009) and Li and Gu (2006) are both adopted.

5.1 Classic galloping

If fixing the rivulet on the cable surface (a_m=0), the phenomenon of RWIVs of stay cable can be simply explained by the mechanism of classic galloping. It is a convenient way to verify the computational program crafted in this paper by means of studying the classic galloping responses. Fig. 8 gives the variations of the cable amplitudes at midpoint with wind velocities when the rivulet is fixed on cable surface at $\gamma+\theta_0$=65.9°, 80.2° and 97.0°. The results of C_D and C_L of stay cable in Gu *et al*. (2009) are used. From Fig. 5, a sudden decrease of C_L, which is regarded as the key factor of galloping, is observed within the range of $\gamma+\theta_0$=63.2°~67.2°. The results in Fig. 8 indicate that a classical galloping vibration takes place when $\gamma+\theta_0$=65.9°, which falls into the range of the sudden decrease of C_L. When $\gamma+\theta_0$=80.2° and 97.0°, which fall out of the range of the sudden decrease of C_L, the stay cable seems to be aerodynamically stable, and no large amplitude vibrations can be found.

5.2 In-plane and out-of-plane cable responses

In this section, the rivulet is assumed to form on all cross sections along the cable axis, and its moving frequency equals to the first natural frequency of the cable. Furthermore, the approaching flow is uniform, which means wind velocities do not vary along the cable axis. Fig. 9 shows the relationship between the in-plane cable amplitudes at midpoint and wind velocities. It can be found from Fig. 9 that cable vibrations have limited amplitude within limited wind velocity range (from 5 m/s to 15 m/s), which is regarded as the main feature of RWIVs of stay cable. Maximum cable amplitude computed by using C_D, C_L from Gu *et al.* (2009), 0.43 m, is larger than that from Li and Gu (2006), 0.28 m.

Displacement time histories of the cable at midpoint and its corresponding power spectral densities for U_0=7 m/s and 10 m/s are given in Fig. 10. C_D, C_L from Gu *et al.* (2009) are used. It can be found from Fig. 10 that only the first natural frequency of stay cable, 0.415 Hz, are activated when the rivulet forms on all cross sections along the cable axis and moves up and down with a frequency equal to the cable fundamental frequency.

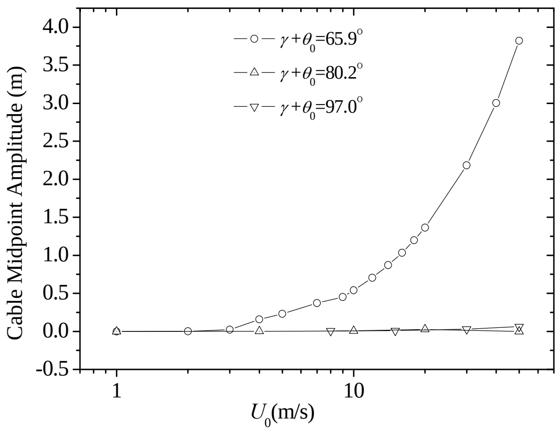

Fig. 8 Classic galloping responses

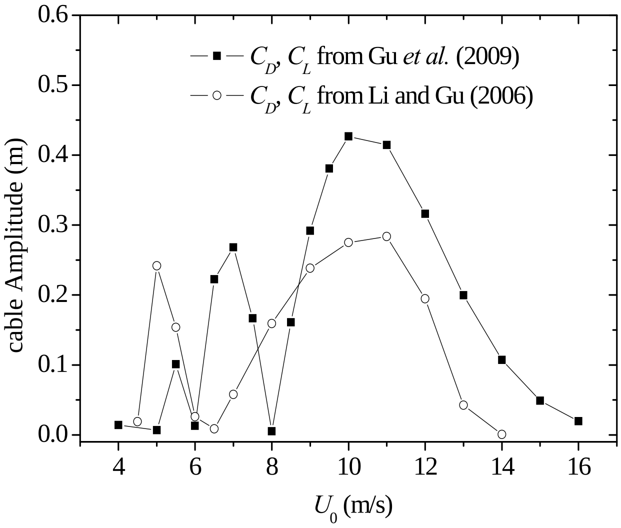

Fig. 9 The relationship between the in-plane cable amplitudes at midpoint and wind velocities

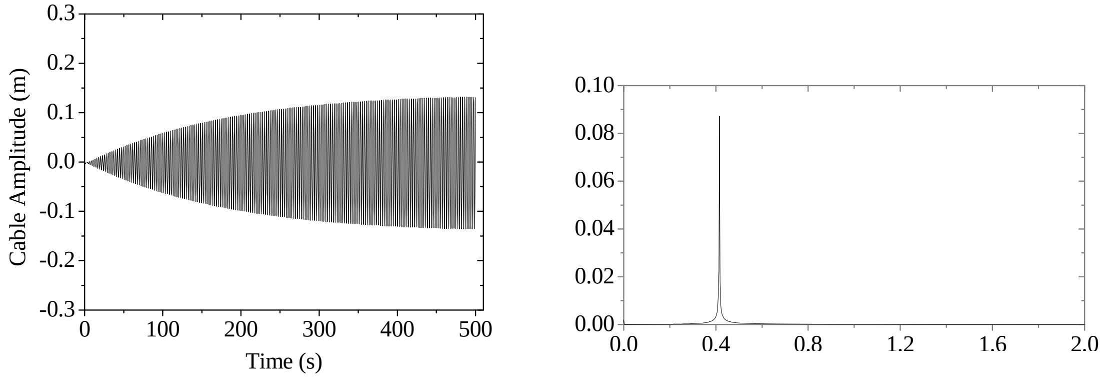

U_0=7.0 m/s

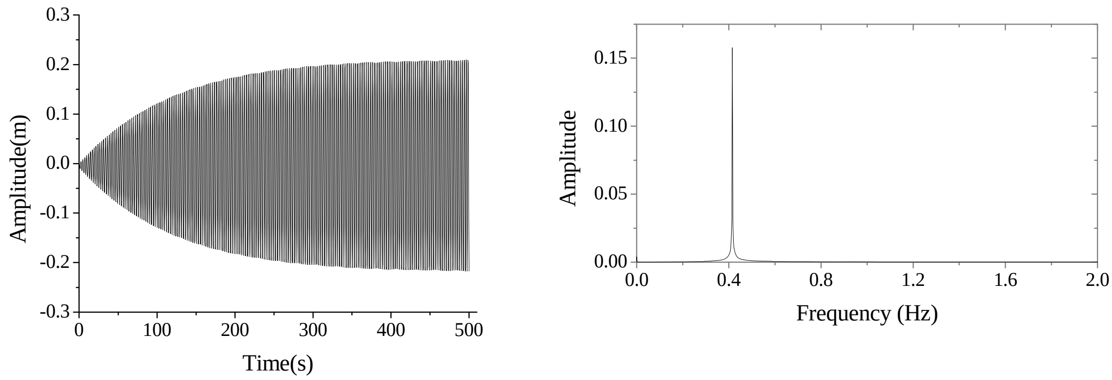

U_0=10.0 m/s

Fig. 10 Displacement time histories and the corresponding power spectral densities of the cable at midpoint for U_0=7 m/s and 10 m/s (C_D, C_L from Gu *et al.* (2009))

The studies on RWIV of stay cable in wind tunnel tests and theoretical analyses usually focus on the in-plane vibration. However, the out-of-plane cable vibration, together with in-plane vibration, was observed in prototype bridges (Chen *et al.* 2004). Fig.11 presents the relationship between the in-plane and out-of-plane oscillation displacements at the midpoint of stay cable. Wind velocity is 10 m/s, and the result of C_D, C_L from Gu *et al.* (2009) is used. It can be found from Fig. 11 that the in-plane amplitude is much greater than the out-of-plane amplitude, which seems to agree well with the results from field observations (Hikami and Shiraishi 1988, Chen *et al*. 2004).

5.3 Effects of rivulet frequencies

In wind tunnel tests to recur RWIVs of stay cables, the rivulet frequency was observed to be identical with the frequency of segmental cable model, which is a single degree-of-freedom system. But for a continuous stay cable, a few natural frequencies of stay cable, for example the 1^{st} ~4^{th}, could be activated in RWIVs. The rivulet frequency may be equal to any natural frequency of stay cable when RWIV takes place.

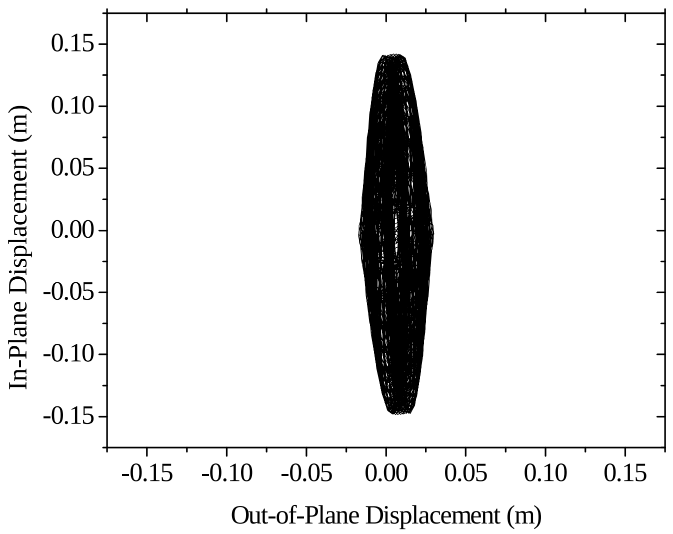

Fig. 11 The relationship between the in-plane and out-of-plane oscillation displacements at the midpoint of stay cable (U_0=10m/s, C_D, C_L from Gu *et al.* (2009))

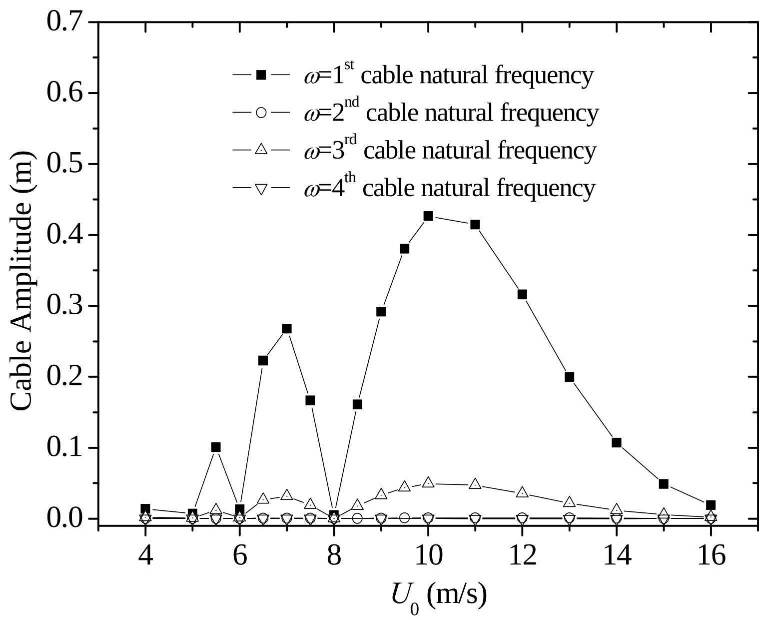

Fig. 12 Effects of the rivulet frequencies to cable amplitude

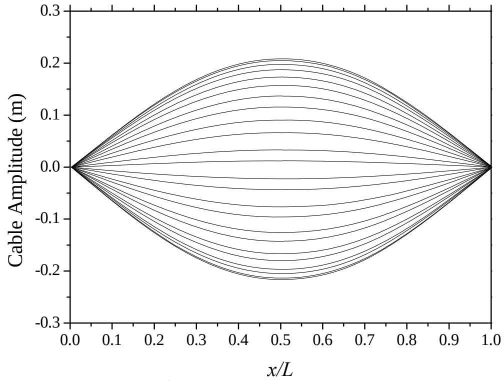

(a) ω=1st cable natural frequency

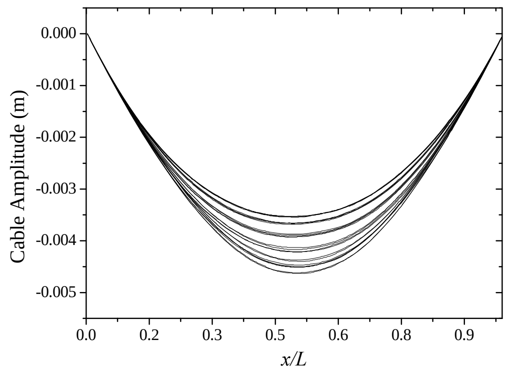

(b) ω=2nd cable natural frequency

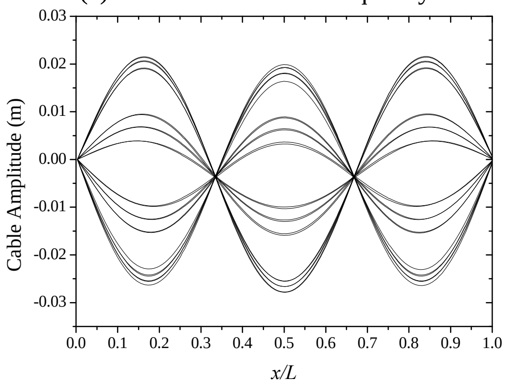

(c) ω=3rd cable natural frequency

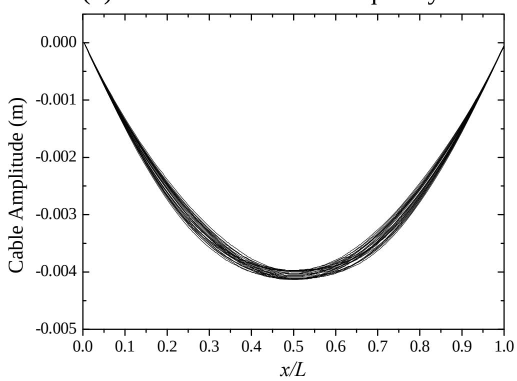

(d) ω=4th cable natural frequency

Fig. 13 The oscillation configuration of the cable when the rivulet frequency is equal to the 1st, 2nd, 3rd and 4th natural frequencies of the stay cable (U_0=10 m/s)

Fig. 12 describes the cable amplitudes when the rivulet frequency is equal to the 1st, 2nd, 3rd and 4th natural frequencies of the stay cable. Fig. 13 shows the oscillation configuration of the cable when the rivulet frequency is equal to the 1st, 2nd, 3rd and 4th natural frequencies of the stay cable (U_0=10 m/s). Notice that the rivulet is assumed to form on all cross sections along the cable axis, and the approaching flow is uniform. It can be found from Fig. 12 that the largest cable amplitude happens when the rivulet frequency is equal to the 1st cable natural frequency. When the rivulet frequency is identical with the 3rd cable natural frequency, cable's vibration is rather obvious, but much less than that of the 1st cable natural frequency. However, when the rivulet frequency is equal to the 2nd or 4th cable natural frequencies, it seems that the stay cable keeps aerodynamically stable. From Fig. 13, it can be seen that the 1st and 3rd cable mode shapes can be activated, but the 2nd and 4th cable mode shapes can't be activated when the rivulet is assumed to form on all cross sections along cable axis. This is because the aerodynamic forces acting on the cable are uniform along the cable axis if the rivulet is assumed to form on all cross sections along the cable axis. The works of this kind of forces on the 2nd and 4th cable mode shapes are zero at any time. However, for the 1st and 3rd cable mode shapes, the works of the aerodynamic forces along the cable axis may be positive.

5.4 Effects of rivulet distribution along cable axis

The rivulet may only exist on a part of cross sections along cable axis, for example, half-span and quarter-span as shown in Fig. 14, which will play an important role on the responses of RWIVs. Fig. 15 gives the relationship between in-plane cable amplitude and wind velocity when the rivulet distributes on half-span of the cable. Fig. 16 shows the oscillation configurations of the cable when the rivulet distributes on half-span of the cable (U_0=10 m/s). Notice that the approaching flow is uniform. It can be found from Fig. 15 that large amplitude of cable vibration can be observed when rivulet frequency is equal to the 2nd (besides 1st and 3rd) natural frequency of stay cable, which is different from the results when the rivulet forms on all cross sections along cable axis. The 2nd cable mode shape can be activated when the rivulet forms on half-span of the cable. However, the 4th cable mode shape of the cable still keeps calm under this case, as can be seen in Fig. 16. On the basis of above results, it can be deduced that the 4th cable mode shape can be activated if the rivulet only forms on quarter-span of the cable, which is verified by the numerical simulations, as shown in Fig. 17.

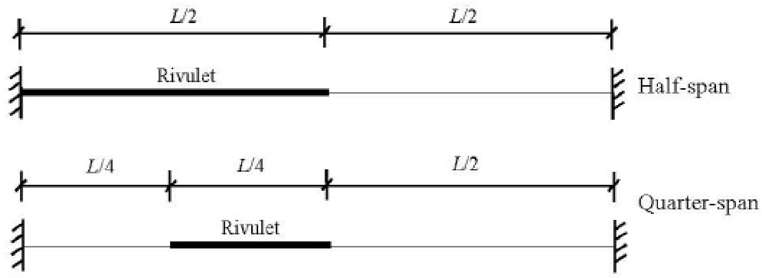

Fig. 14 Diagram of rivulet distribution along cable axis (half-span and quarter-span)

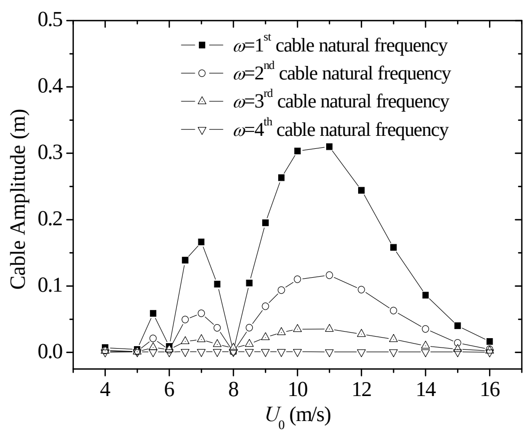

Fig. 15 The relationship between cable amplitudes and wind velocity under different rivulet frequencies (half-span rivulet)

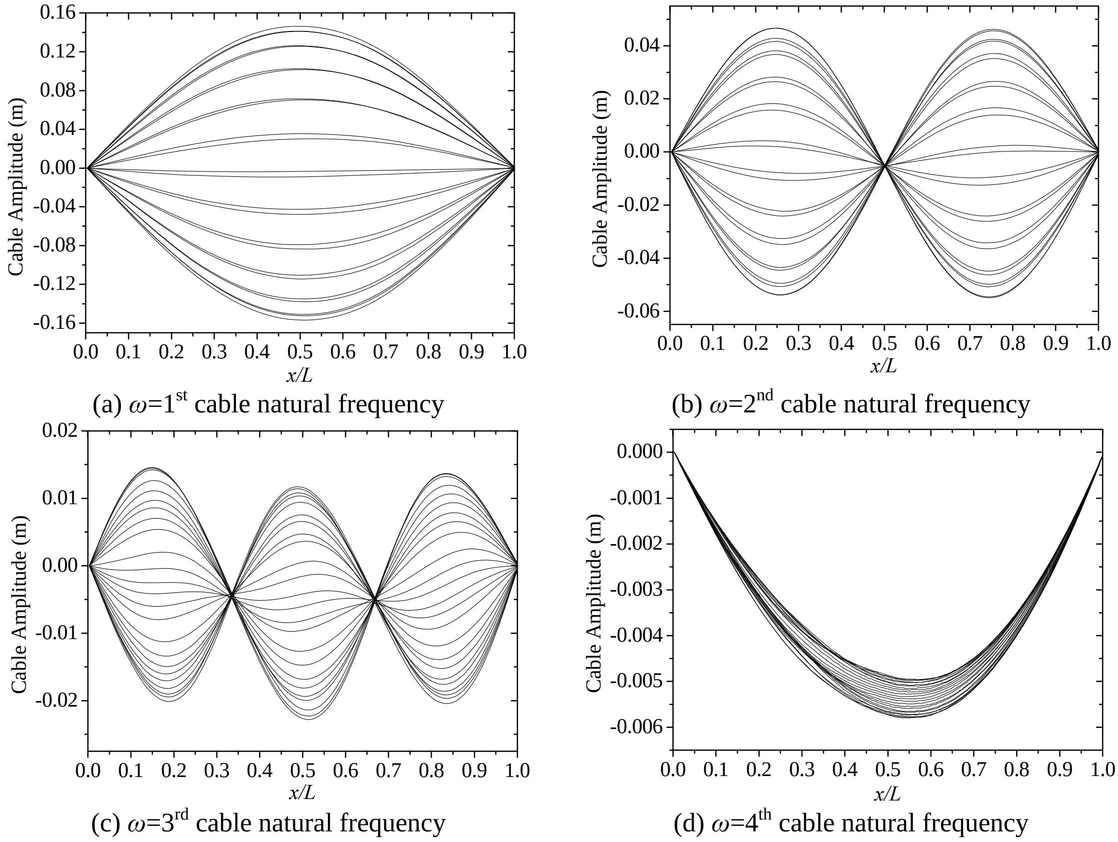

(a) ω=1st cable natural frequency (b) ω=2nd cable natural frequency

(c) ω=3rd cable natural frequency (d) ω=4th cable natural frequency

Fig. 16 The oscillation configuration of the cable for half-span rivulet (U0=10 m/s)

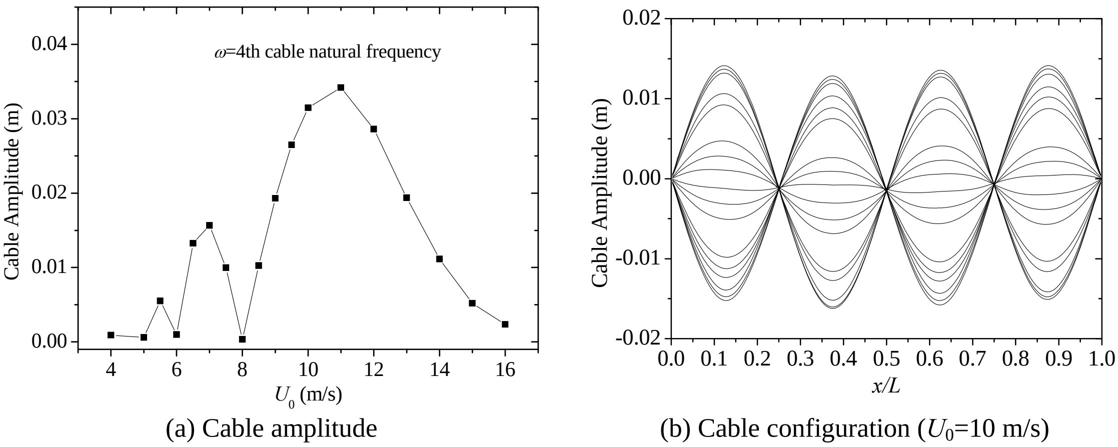

(a) Cable amplitude (b) Cable configuration (U_0=10 m/s)

Fig.17 Cable amplitude and configuration for quarter-span rivulet when the rivulet equals to 4th cable natural frequency

5.5 Effects of mean wind velocity profile

Mean wind velocity at atmospheric boundary layer increases with the height over the ground, which usually is described by power law or logarithmic law in some Standards and Codes. Terrain category B of Chinese Code GB50009-2012 is used, in which the mean wind velocity is expressed as power law. For terrain category B, the mean wind velocity at the height of z, $U(z)=U_{10}(z/10)^{0.15}$ (U_{10} is basic wind speed). The bridge deck level is selected to be reference height of wind velocity. Fig. 18 shows the variation of the in-plane cable amplitude and wind velocity when the rivulet frequency is respectively equal to the 1st, 2nd, 3rd and 4th natural frequencies of the cable. Notice that the rivulet forms on all cross sections along cable axis. Similar to uniform approaching flow, the cable amplitude when rivulet frequency is equal to the 1st cable natural frequency is much larger than those of three other cases, as indicated in Fig. 18. However, four cable mode shapes can all be activated under the case of full-span rivulet at specific wind velocity at deck level, which is different from the result in uniform approaching flow, as shown in Fig. 19. It is because that the rivulet equilibrium position, θ_0, varies with cable cross sections at different height, and only a part of θ_0 falls into the sudden decrease of C_L.

5.6 Effects of the damping of stay cable

The variation of the in-plane cable amplitudes with damping ratios of stay cable is shown in Fig. 20. It can be found from Fig. 15 that the amplitude of the cable decreases with the increase of cable damping ratio. It seems that RWIVs of stay cables can be well mitigated when damping ratio of stay cable is higher than 1%.

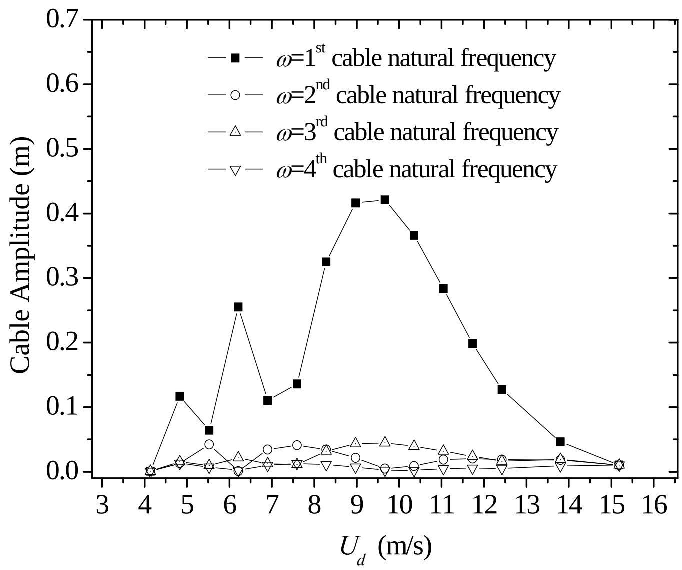

Fig. 18 Effect of mean wind velocity profile

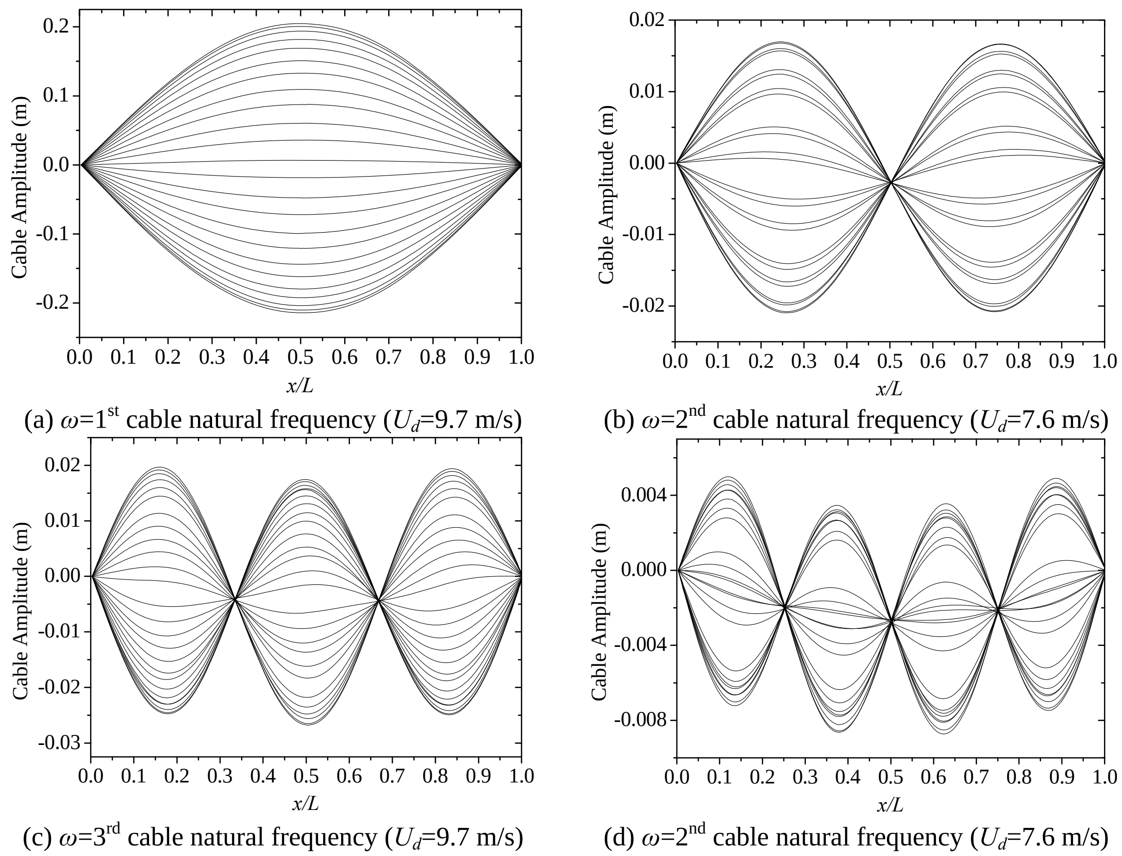

Fig. 19 The oscillation configuration of the cable for full-span rivulet (Terrain category B of Chinese Code GB50009-2012)

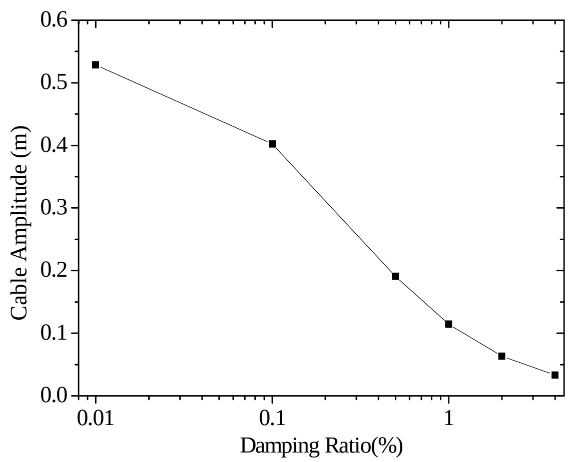

Fig. 20 The relation between cable amplitudes and damping ratios

6. Conclusions

The equations of motion of a continuous stay cable suffering from RWIVs are derived in a Cartesian Coordinate System by neglecting high order terms, which is acceptable for the small sag of stay cable. Some parameters, including cable static profile, aerodynamic forces on stay cable and motion law of the rivulet are discussed in detail. Then, finite difference method is utilized to solving the equations of motion of the continuous stay cable to obtain the responses of RWIVs, and the corresponding computational program is crafted. The results show that the stay cable exhibits classic galloping characteristics if fixing the rivulet on the cable surface within the sudden decrease zone of lift coefficient, which gives evidence to validate the effectiveness of the computational program. The RWIV responses are carefully investigated by assuming the rivulet forming on full-span of the cable and moving with a frequency equal to the 1^{st}, 2^{nd}, 3^{rd}, 4^{th} cable natural frequency, respectively. The results indicate that limited cable amplitudes are achieved within a limited range of wind velocity, which meets the RWIV characteristics. It appears that in-plane cable amplitude is much larger than out-of-plane cable amplitude. However, the even order natural frequencies of the cable seem to be hard to be activated if the rivulet forms on full-span of the cable. The effects of rivulet distribution along cable axis are systematically studied by assuming the rivulet forms on half-span and quarter-span of the cable. The results indicates that the 2^{nd} cable natural frequency can be activated by half-span rivulet, and the 4^{th} cable natural frequency can be activated by quarter-span rivulet. Uniform flow is used in the above investigations. Numerical simulations based on terrain category B of Chinese Code GB50009-2012 presents that the 1^{st}~4^{th} cable natural frequencies can all be activated at certain wind velocities, even if the rivulet forms on full-span of the cable. Finally, the effects of damping ratio on RWIV of stay cable are carefully investigated, which suggests that damping ratio of 1% is needed to well mitigate RWIVs of stay cables.

Ackownledgments

This project was jointly supported by the National Basic Research Program of China (973 Program: 2015CB057701 and 2015CB057702), the National Natural Science Foundation (50708035), the China Postdoctoral Science Foundation (20060400873), to which the authors gratefully appreciate.

References

Burgh A.H.P. and van der, Hartono (2003), "Rain-wind-induced vibrations of a simple oscillator", *Int. J. Nonlinear Mech*., **39**(1), 93-100.

Cao, D.Q., Tucker, R.W. and Wang, C. (2003), "A stochastic approach to cable dynamics with moving rivulets", *J. Sound Vib*., **268**(2), 291-304.

Chen, Z.Q., Wang, X.Y., Ko, J.M., Ni, Y.Q., Spencer, B.F., Yang, G. and Hu, J.H. (2004), "MR damping system for mitigating wind-rain induced vibration on Dongting Lake cable-stayed bridge", *Wind Struct*., **7**(5), 293-304.

Cosentino, N., Flamand, O. and Ceccoli, C. (2003), "Rain-wind induced vibration of inclined stay cables. Part Ⅱ: Mechanical modeling and parameter characterization", *Wind Struct*., **6**(6), 485-498.

Gu, M. (2009), "On wind-rain induced vibration of cables of cable-stayed bridges based on quasi-steady assumption", *J. Wind Eng. Ind. Aerod.*, **97**(7-8), 381-391.
Gu, M. and Du, X.Q. (2005), "Experimental investigation of rain-wind-induced vibration of cables in cable-stayed bridges and its mitigation", *J. Wind Eng. Ind. Aerod.*, **93**(1), 79-95.
Gu, M., Du, X.Q. and Li, S.Y. (2009), "Experimental and theoretical simulations on wind–rain-induced vibration of 3-D rigid stay cables", *J. Sound Vib.*, **320**(1-2), 184-200.
Gu, M., Liu, C.J., Xu, Y.L. and Xiang, H.F. (2002), "Response characteristics of wind excited cables with artificial rivulet", *Appl. Math. Mech*., **23**(10), 1176-1187.
Gu, M. and Lu, Q. (2001), "Theoretical analysis of wind-rain induced vibration of cables of cable-stayed bridges", *J. Wind Eng*., **89**, 125-128.
Hikami, Y. and Shiraishi, N. (1988), "Rain-wind induced vibrations of cables in cable stayed bridges", *J. Wind Eng. Ind. Aerod.*, **29**(1-3), 409-418.
Holmes, J.D. (2003), *Wind loading of structures*, Spon press.
Irvine, H.M. (1981), *Cable Structure*, the MIT Press.
Li, H., Chen W.L., Xu, F., Li, F.C. and Ou, J.P. (2010), "A numerical and experimental hybrid approach for the investigation of aerodynamic forces on stay cables suffering from rain-wind induced vibration", *J. Fluid Struct*., **26**(7-8), 1195-1215.
Li, S.Y., Chen, Z.Q., Kareem, A. and Wu, T. (2013), "On the rain-wind induced in-plane and out-of-plane vibrations of stay cables", *J. Eng. Mech. -ASCE*, **139**(12), 1688-1698.
Li, S.Y. and Gu, M. (2006), "Numerical simulations of flow around stay cables with and without fixed artificial rivulets", *Proceedings of the 4th International Symposium on Computational Wind Engineering (CWE2006)*,Yokohama, Japan.
Matsumoto, M., Saitoh, T., Kitazawa, M., Shirato, H. and Nishizaki, T. (1995), "Response characteristics of rain-wind induced vibration of stay-cables of cable-stayed bridges", *J. Wind Eng. Ind. Aerod.*, **57**(2-3), 323-333.
Matsumoto, M., Shirato, H., Yagi, T., Goto, M., Sakai, S. and Ohya, J. (2003), "Field observation of the full-scale wind induced cable vibration", *J. Wind Eng. Ind. Aerod.*, **91**(1-2), 13-26.
Peil, U. and Nahrath, N. (2003a), "Modeling of rain-wind induced vibrations", *Wind Struct*., **6**(1), 41-52.
Peil, U., Nahrath, N. and Dreyer, O. (2003b), *Modeling of rain-wind induced vibrations*, 11ICWE, Lubbock, USA.
Ren, S.Y. and Gu, M. (2005), "Static analysis of cables' configuration in cable-stayed bridges", *J. Tongji Univ*., **33**(5), 595-599. (in Chinese)
Rocchi, D. and Zasso, A. (2002), "Vortex shedding from a circular cylinder in a smooth and wired configuration: comparison between 3D LES simulation and experimental analysis", *J. Wind Eng. Ind. Aerod.*, **90**(4-5), 475-489.
Taylor, I.J. and Robertson, A.C. (2011), "Numerical simulation of the airflow-rivulet interaction associated with the rain-wind induced vibration phenomenon", *J. Wind Eng. Ind. Aerod.*, **99**(9), 931-944.
Wilde, K. and Witkowski, W. (2003), "Simple model of rain-wind-induced vibrations of stayed cables", *J. Wind Eng. Ind. Aerod.*, **91**(7), 873-891.
Xu, Y.L., Chen, J., Ng, C.L. and Zhou, H.J. (2008), "Occurrence probability of wind-rain-induced stay cable vibration", *Adv. Struct. Eng*., **11**(1), 53-69.
Xu, Y.L. and Wang, L.Y. (2003), "Analytical study of wind-rain-induced cable vibration: SDOF model", *J. Wind Eng. Ind. Aerod.*, **91**(1-2), 27-40.
Yamaguchi, H. (1990), "Analytical study on growth mechanism of rain vibration of cables", *J. Wind Eng. Ind. Aerod.*, **33**(1-2), 73-80.
Zhou, H.J. and Xu, Y.L. (2007), "Wind-rain-induced vibration and control of stay cables in a cable-stayed bridge", *Struct. Control Health Monit*., **14**(7), 1013-1033.

CC